Rapid Communications

Strongly fluctuating moments in the high-temperature magnetic superconductor $RbEuFe_4As_4$

K. Willa,[1] R. Willa,[1] J.-K. Bao,[1] A. E. Koshelev,[1] D. Y. Chung,[1] M. G. Kanatzidis,[1,2] W.-K. Kwok,[1] and U. Welp[1]
[1]*Materials Science Division, Argonne National Laboratory, 9700 South Cass Avenue, Lemont, Illinois 60439, USA*
[2]*Department of Chemistry, Northwestern University, Evanston, Illinois 60208, USA*

(Received 2 November 2018; revised manuscript received 1 March 2019; published 23 May 2019)

The iron-based superconductor $RbEuFe_4As_4$ undergoes a magnetic phase transition deep in the superconducting state. We investigate the calorimetric response of $RbEuFe_4As_4$ single crystals of the magnetic and the superconducting phase and its anisotropy to in-plane and out-of-plane magnetic fields. Whereas the unusual cusplike anomaly associated with the magnetic transition is suppressed to lower temperatures for fields along the crystallographic c axis, it rapidly transforms to a broad shoulder shifting to higher temperatures for in-plane fields. We identify the cusp in the specific-heat data as a Berezinskii-Kosterlitz-Thouless transition with fine features caused by the three-dimensional effects. The high-temperature shoulder in high magnetic fields marks a crossover from a paramagnetically disordered to an ordered state. This observation is further supported by Monte Carlo simulations of an easy-plane two-dimensional Heisenberg model and a fourth-order high-temperature expansion, both of which agree qualitatively and quantitatively with the experimental findings.

DOI: 10.1103/PhysRevB.99.180502

While superconductivity and magnetic order usually are mutually exclusive due to their competitive nature, a series of novel materials that feature the coexistence of both phases has recently emerged [1–3]. In order to address open questions on the coexistence/interplay/competition between these two phases of matter, it is crucial to study model systems, where both phenomena can be tuned independently from each other. The Eu-based pnictide superconductors—where superconductivity occurs within the Fe_2As_2 layers, while the magnetism is hosted by the Eu^{2+} ions—provides such a model system [3]. Furthermore, each phenomenon appears to be relatively robust against perturbing the other one. In fact, chemical substitution of the parent nonsuperconducting compound $EuFe_2As_2$, e.g., with P (on the As site), K, or Na (on the Eu site) induces superconductivity [4–6] (with a maximum T_c of 23, 30, and 35 K, respectively), while only smoothly suppressing the magnetic order temperature $T_m \sim 19$ K. Recent syntheses [7,8] of members of the 1144 family ($CsEuFe_4As_4$ and $RbEuFe_4As_4$ with T_c in the mid-30-K range) have opened new possibilities to tune the separation, and hence the interaction between neighboring Eu layers.

In this Rapid Communication we report a detailed calorimetric characterization of single-crystal $RbEuFe_4As_4$: In particular, we investigate the anisotropic response near the magnetic phase transition at $T_m = 14.9$ K (well within the superconducting state, $T_c = 37$ K) to external fields. Whereas earlier studies on polycrystalline samples [8] have suggested that the magnetic transition might be of third (higher-than-second) order, we demonstrate that the behavior of the specific heat is broadly consistent with a Berezinskii-Kosterlitz-Thouless (BKT) [9–11] transition with the europium moments confined to the plane normal to the crystallographic c axis by crystal anisotropy. This finding is based on two main observations: First, the variation of the specific heat C in the vicinity of the phase transition agrees qualitatively and quantitatively with that of a BKT transition. In particular, the BKT scenario naturally explains the absence of a singularity at the transition point. Second, the anisotropic response of the specific heat to different field directions clearly points towards a strong ordering of the moments within the Eu planes. The reported findings are supported by numerical Monte Carlo simulations of a classical anisotropic two-dimensional (2D) Heisenberg spin system.

Generally, a BKT transition separates a high-temperature phase consisting of a liquid of magnetic vortices and antivortices from a low-temperature phase where only bound vortex-antivortex pairs are present. In a truely 2D case the average magnetic moment would thus be destroyed by spin-wave fluctuations even in the ordered phase. Weak interlayer coupling, as present in $RbEuFe_4As_4$, promotes a small average in-plane moment formed at very large scales, while at smaller scale the behavior remains two dimensional. As a result the true phase transition in this system belongs to the universality class of the three-dimensional (3D) anisotropic Heisenberg model. However, these 3D effects are only relevant within a narrow range near the transition temperature and add fine features modifying the overall 2D behavior. Similar scenarios are realized in several layered magnetic compounds, such as K_2CuF_4 [12,13] and Rb_2CrCl_4 [14,15].

The appearance of the superconducting phase below $T_c = 36.8(6)$ K and a magnetic phase below $T_m = 14.9$ K is clearly revealed in the calorimetric data (for measurement details please refer to Supplemental Material A [16] and Refs. [17,18]) obtained on zero-field cooling from room temperature down to 2 K (see Fig. 1). Whereas the superconducting transition temperature is extracted through an entropy conserving construction [see Fig. 1(f)], we determine the magnetic transition temperature from the position of the specific-heat cusp, which does not show signs of a first- or second-order phase transition. This observation is in line with previously reported results on polycrystalline $CsEuFe_4As_4$ [7] and $RbEuFe_4As_4$ [8], and should be contrasted to results on

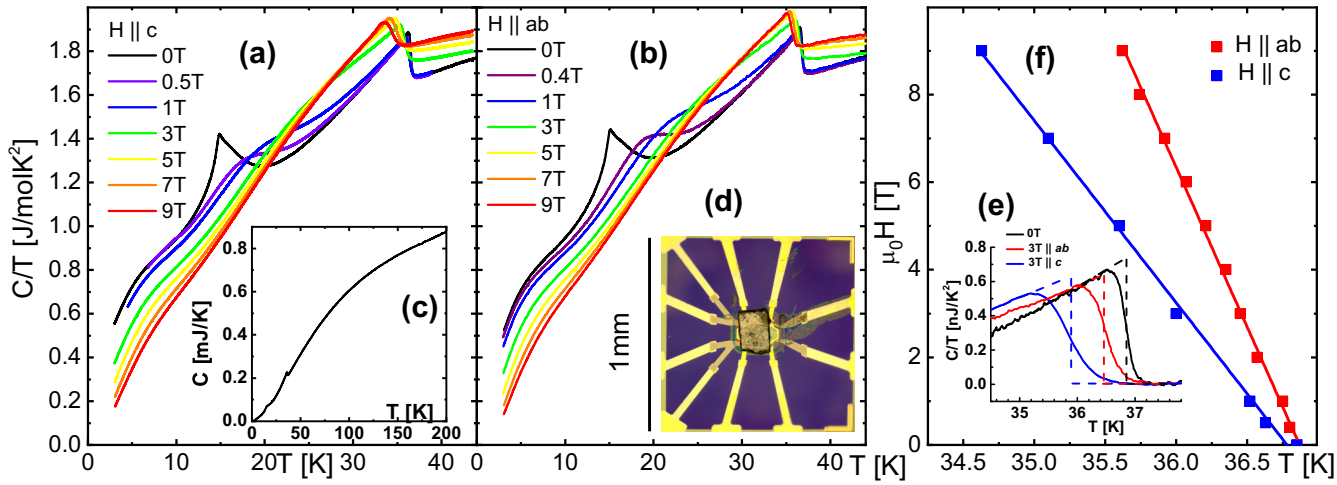

FIG. 1. Entropy change (C/T) in single-crystal $RbEuFe_4As_4$ and its dependence on the magnetic field strength when applied (a) along and (b) perpendicular to the crystallographic c axis. The superconducting transition at $T_c = 37$ K and the magnetic transition at 15 K are clearly visible in the zero-field calorimetric scan (c), as obtained from a room-temperature cooldown. The microscope image (d) shows the ac nanocalorimeter platform with a $RbEuFe_4As_4$ single crystal mounted at its center. Following the evolution of the superconducting transition in an applied field, (e), allows one to extract the phase diagram (f) and to evaluate the superconducting anisotropy $\Gamma = 1.8$. The apparent discrepancy in the extrapolated T_c is within the experimental uncertainty.

$EuFe_2As_2$ which show a singularity [19–22]. The variation of the specific heat in the vicinity of the phase transition can be expressed [23] as $C = a^{\pm}|t|^{-\alpha} + b(t)$. The first term captures the critical behavior near $t = 0$ with $t = T/T_m - 1$ the reduced temperature, $a^{\pm}$ the critical amplitudes for $t < 0$ $(-)$ and $t > 0$ $(+)$, and α the critical exponent. The second term captures all regular contributions (e.g., from phonons) and is typically modeled by a linear form $b(t) = b_0 + b_1 t$ in a small temperature range around the transition. A nondivergent specific heat implies $\alpha < 0$, and hence the constant $b_0 \equiv C(T_m)$ assumes the value of the specific heat at the transition temperature. For each branch $t \lessgtr 0$, we find a critical exponent $\alpha \approx -1$, a highly unusual value. For the critical amplitudes we find $a^+ = 18.5$ J/mol K and $a^- = 4.76$ J/mol K, respectively (see fits in Fig. 2).

Contrary to earlier speculations [8], we find that this transition with nonsingular behavior is consistent with a Berezinskii-Kosterlitz-Thouless transition of the Eu^{2+} magnetic moments weakly influenced by 3D effects. A uniaxial anisotropy forces the moments to orient within the crystallographic ab plane, effectively reducing the moment's degrees of freedom to that of a 2D XY spin system. A more detailed justification shall be given below. The down-bending of the calorimetric data below ~10 K is attributed to the quantum nature of the high-spin Eu^{2+} moments [24–26]. In applied fields, the superconducting transition temperature is gradually suppressed; the effect is stronger if the field is applied along the c axis. The rate of T_c suppression, $dT_c/dH|_{ab} = 0.14$ K/T and $dT_c/dH|_c = 0.25$ K/T, provides a uniaxial *superconducting* anisotropy of $\Gamma = 1.8$, as shown in Fig. 1. These values agree with complementary magnetization and transport measurements [26,27] on single-crystal $RbEuFe_4As_4$. No influence on the step height $\Delta C/T$ or the phase boundary from magnetism is detected in fields up to 9 T. In high fields, $0.4\ \text{T} < \mu_0 H < 9\ \text{T}$, the cusp of the magnetic transition evolves into a broad magnetic hump with its center moving to higher temperatures. At the highest field (9 T) these magnetic fluctuations extend up to about 100 K—far above the superconducting transition—and provide a natural explanation for the reported negative, normal-state magnetoresistance [26]. We attribute this hump to a field-induced polarization of the Eu^{2+} moments along the field direction and their associated fluctuations.

For a more detailed analysis of the magnetic transition, we performed low-field calorimetric scans in the vicinity of T_m. Given the robust superconductivity (low dT_c/dH) and the clear separation of energy scales $k_B T_m \ll k_B T_c$, the low-field changes in the calorimetric data can be attributed to the magnetism. To accentuate these, we have to subtract an overall background. However, subtracting a phonon-type background turns out to be difficult because of other (in particular, superconducting) contributions. We therefore subtract the 9-T specific-heat data (field along the c axis). While the latter still contains magnetic and superconducting contributions, both are essentially featureless in the temperature range of interest (see Fig. 1). As shown in Fig. 2, for small applied fields along the c axis, the specific-heat cusp at the magnetic transition shifts to lower temperatures while broadening slightly and a shoulder in the specific heat appears on the high-temperature side. Defining the phase boundary $T_m(H)$ as the position of the cusp (see Fig. 3), a mean-field fit provides the empiric law $T_m(H) = T_m[1 - (H/H_0)^2]$, with $\mu_0 H_0 \approx 0.93$ T. This suggests that at this field value the planar anisotropy is overcome at all temperatures, i.e., at zero temperature the magnetic moments fully align with the field normal to the ab plane. A comparable saturation field can be deduced from low-temperature magnetization curves [26]. For in-plane fields, the position of the cusp is almost field independent, while its size is readily suppressed (disappearing at 0.14 T) and a pronounced shoulder appears on the high-temperature side. As discussed below, we attribute the cusp to a weak 3D coupling between Eu layers. The appearance of the high-temperature

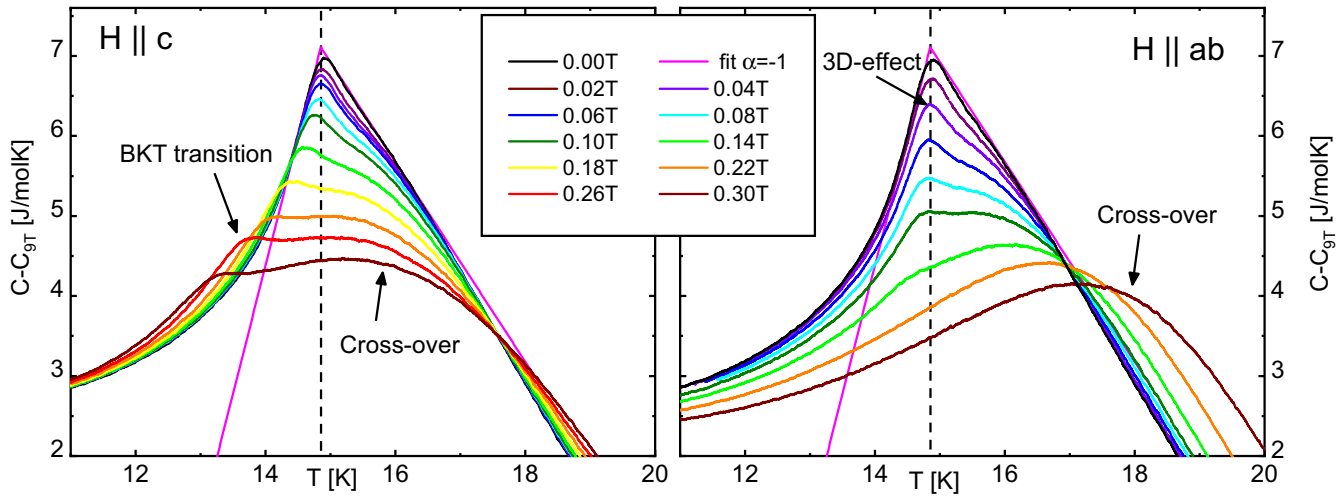

FIG. 2. Specific heat subtracted by the 9-T background curve around the magnetic transition upon applying fields from 0.02 to 0.3 T out of plane (left) and in plane (right). The sharp kink indicating the ordering of the Eu^{2+} moments in the plane while the broad hump developing at higher temperatures shows the gradual magnetization of the sample parallel to the applied field.

feature marks the onset of magnetic polarization, as discussed above. This hump is not a sharp phase boundary but should rather be understood as a crossover from a paramagnetically disordered to an ordered state. Due to anisotropy effects, this occurs more rapidly for in-plane than for out-of-plane fields.

Further insight into the response of $RbEuFe_4As_4$ is gained through a detailed study of a model spin system describing the key features of this compound, implemented using a Monte Carlo [28,29] algorithm (see Supplemental Material B [16]). More specifically, we have investigated the magnetic and thermodynamic properties of a two-dimensional square lattice of [Heisenberg-type, $O(3)$] classical spins $\boldsymbol{s}_i$ governed by the Hamiltonian

$$\mathcal{H} = -J\sum_{\langle i,j\rangle}\boldsymbol{s}_i\boldsymbol{s}_j + K\sum_i\left(2s_{i,z}^2-1\right) - \boldsymbol{h}\sum_i\boldsymbol{s}_i. \quad (1)$$

Here, J defines the isotropic coupling between nearest-neighbor spin pairs $\langle i,j\rangle$, and K introduces a uniaxial anisotropy in spin space. The last term describes the coupling to an external magnetic field $\boldsymbol{h}$. Without limiting the generality of the foregoing, we set $|\boldsymbol{s}_i| = 1$. A similar approach has been extensively used in the past to explore the 2D XY model (see Refs. [30–34]).

The simulated system is purely two dimensional, and hence neglects the coupling between neighboring Eu layers. This choice is motivated by the observation that the parent nonsuperconducting compound $EuFe_2As_2$ displays small interlayer interactions compared to the intralayer interactions. We expect the coupling between Eu layers to be even weaker in $RbEuFe_4As_4$, as the separation between Eu layers doubled and two superconducting layers are in between. The interlayer coupling becomes relevant only at temperatures near the transition and for small magnetic fields. In the Hamiltonian (1), the spin anisotropy is modeled by a crystalline term $\propto s_{i,z}^2$. The Eu^{2+} ions have a vanishing angular momentum ($L = 0$), which excludes a crystalline anisotropy originating from spin-orbit coupling. However, the coupling between the Eu^{2+} moments and Fe d electrons—the latter are known to feature an easy-plane anisotropy [35,36]—naturally leads to such a term (see Supplemental Material D [16]). Other sources of anisotropy such as dipolar interactions, considered elsewhere [37], are neglected. The anisotropic term causes the system to fall into the universality class of 2D XY spin systems, where a BKT transition is known to occur at a finite temperature $T_m > 0$ [38]. In contrast to our model, an isotropic (in spin space) 3D Heisenberg model with anisotropic nearest-neighbor coupling (J in plane versus $J' = \lambda J$ between Eu layers) fails to capture an anisotropic susceptibility, while the isotropic (in spin space) two-dimensional Heisenberg model does not undergo a phase transition at finite temperatures [39–42].

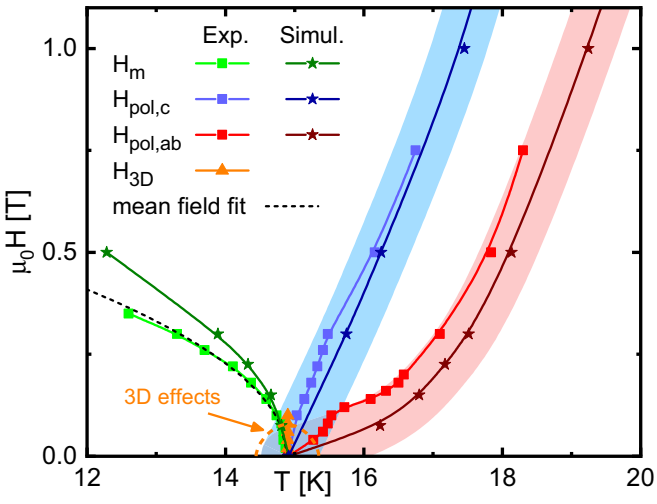

FIG. 3. Boundaries of the magnetic phase as obtained from measured and simulated calorimetric data. The transition to an ordered magnetic phase is shown by green symbols, and agrees well with the empiric law $H_m = H_0(1 - T/T_m)^{1/2}$, when the field is applied along the c axis. A broad hump in the specific heat marks the crossover to a field-driven polarized state of Eu^{2+} moments and is shown for fields parallel (blue) and normal (red) to the c axis.

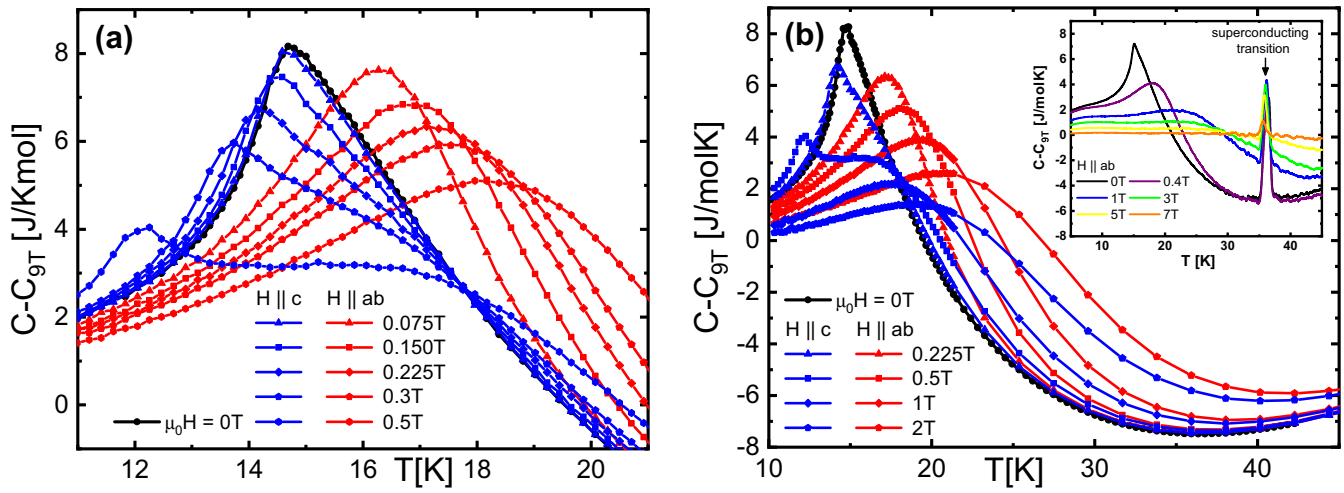

FIG. 4. Simulated specific heat of the anisotropic 2D Heisenberg spin system and its dependence on temperature for different magnetic fields and their orientations; red (in plane), blue (out of plane), and black (zero field). For all curves the 9-T background data is subtracted [conversion to real units using Eq. (2)]. (a) shows the low-field features and their anisotropic response near the magnetic transition. The specific heat at larger fields, and over a wider temperature range, is shown in (b). The experimental signature of the superconducting transition near 37 K (see inset) is not captured in the simulations.

We investigate several response functions in this system: the (direction-dependent) magnetic susceptibility $\chi_\alpha(T)$ ($\alpha = x, y, z$), the specific heat $C(T, \boldsymbol{h})$, the total magnetization $\boldsymbol{S}(T, \boldsymbol{h}) = \sum_i \boldsymbol{s}_i$, and the spin-spin correlation function $G(r) \equiv \langle \boldsymbol{s}(0)\boldsymbol{s}(r)\rangle$. For convenience we introduce the temperature scale $T_0 \equiv J/k_B$. From high-temperature simulations (typically $T/T_0 \in [4, 9]$), we fit the inverse magnetic susceptibility to a Curie-Weiss law $\chi_\alpha^{-1}(T) \propto T - \Theta_{C,\alpha}$ to extract the Curie temperatures $\Theta_{C,\alpha}$. A comparison between the measured and the simulated susceptibility can be found in Supplemental Material C3 [16]. Any nonzero value of K results in an anisotropy between the in-plane ($\Theta_{C,x}$) and out-of-plane ($\Theta_{C,z}$) Curie temperature. By comparing the anisotropy ratio $\Theta_{C,x}/\Theta_{C,z}$ with the reported [26] value of 1.075 for $RbEuFe_4As_4$ obtained from magnetization measurements, we find an agreement for the specific value $K = 0.1J$, where $\Theta_{C,x} = 1.20T_0$ and $\Theta_{C,z} = 1.12T_0$. All further simulations are performed for this anisotropy parameter. The influence of the anisotropy parameter on the shape of $C(T)$ dependence at $h = 0$ and the location of the cusp is considered in Supplemental Material C4 [16].

In zero magnetic field, the simulated specific heat shows a clear cusp at $T_m/T_0 = 0.7$, a value that we identify with the transition temperature $T_m = 14.9$ K of the calorimetric experiment. It is known, however, that the true BKT transition temperature T_{BKT} is slightly below the specific-heat cusp. The correlation function is expected to decay as a power law $r^{-1/4}$ at the transition, providing a value $T_{\mathrm{BKT}} = 0.66T_0$, i.e., about 6% below the cusp in the specific heat. At the same time, the correlation function decays as $G(r) \propto \exp[-r/\zeta(T)]$, with a correlation length $\ln[\zeta(T)] \propto (T - T_{\mathrm{BKT}})^{-1/2}$ that diverges upon approaching the transition from above. Evaluation of $\zeta(T)$ and its singular behavior yields a consistent result (see Supplemental Material C2 [16]).

At finite fields, the calorimetric and magnetic responses strongly depend on the field orientation. For fields applied along the spin plane, the $U(1)$ circular degeneracy is lifted and no BKT transition occurs. The system's response follows a typical ferromagnetic behavior (gradual magnetization upon cooling) reaching a fully ordered state at lowest temperatures. The specific heat gradually broadens and shifts to higher temperatures. On the contrary, a field applied perpendicular to the spin lattice preserves the $U(1)$ rotational symmetry and the BKT transition shifts to lower temperatures. Here, the magnetic field acts as an anisotropic term favoring the spin orientation along the z axis, hence retarding the transition to an in-plane spin orientation. The numerical simulations are in excellent qualitative and quantitative agreement with the experimental data (see Figs. 2 and 4). Additionally, the simulations reproduce the behavior of the magnetization and the susceptibility which is discussed in Supplemental Material C3 [16]. The phase boundaries extracted from the simulation data (converted to appropriate units) are shown in Fig. 3. The green curve corresponds to the suppression of the BKT transition due to a field normal to the spin plane. The two other curves correspond to a crossover where magnetic moments are polarized along the field (blue, $H \| c$ and red, $H \| ab$). The simulation result reproduces the experimental data extremely well, with only minor deviations for low fields along the ab plane. This difference is attributed to 3D effects close to the transition that are not accounted for in the simulations.

Having identified realistic values for the dimensionless parameters T/T_0 (from calorimetry) and K/J (from high-temperature magnetization), we can rewrite the model Hamiltonian in Eq. (1) in a dimensional form

$$\mathcal{H}_{\mathrm{real}} = -\mathcal{J}\sum_{\langle i,j\rangle} \boldsymbol{m}_i \boldsymbol{m}_j + 2\mathcal{K}\sum_i m_{i,z}^2 - \boldsymbol{H}\boldsymbol{M}, \qquad (2)$$

where a constant shift has been omitted. Here, $\boldsymbol{M} = \sum_i \boldsymbol{m}_i$ denotes the total magnetization of the individual constituents $|\boldsymbol{m}_i| \approx 7\mu_B$, $\mathcal{J} = 0.6 \times 10^{-23}$ J/μ_B^2 ($=10\mathcal{K}$) providing the relevant energy scale for the ferromagnetic interactions

(the anisotropy). It is useful to express the simulated fields h in dimensional units via $h \rightarrow \mu_0 H = 4.53h$[T].

The numerical results are backed up by a high-temperature expansion of the model described by Eq. (1) (see Supplemental Material C1 [16]). Here, the anisotropy ratio in the Curie temperature takes the simple form

$$\frac{\Theta_{C,x}}{\Theta_{C,z}} = \frac{1 + K/5J}{1 - 2K/5J}, \tag{3}$$

and yields the value 1.06 for $K = 0.1J$. This relation reiterates that for an easy-plane anisotropy $K > 0$ the ratio of Curie temperatures $\Theta_{C,x}/\Theta_{C,z}$ is larger than unity, whereas an easy-axis system ($K < 0$) has $\Theta_{C,x}/\Theta_{C,z} < 1$. Note that the sign of the anisotropy may change for different Eu-containing compounds. We find that the presumed "high-temperature" range $T/T_0 \in [4, 9]$ (corresponding to 50–200 K) is only captured properly when the high-temperature expansion is taken to quartic order in $\beta\mathcal{H}$ [the susceptibility is expanded to cubic order in $\beta = (k_B T)^{-1}$]. This explains the noticeable discrepancy between the "exact" values $\Theta_{C,x}/T_0 = 4/3 + 4K/15J$ (=1.36) and $\Theta_{C,z}/T_0 = 4/3 - 8K/15J$ (=1.28) obtained in the high-temperature limit and their numerical counterparts 1.20 and 1.12 (see above).

We have assumed that the third dimension, perpendicular to the easy plane, plays a marginal role in the calorimetric response of the magnetic order. A weak coupling $J' = \lambda J$ ($|\lambda| \ll 1$) between ferromagnetically ordered Eu layers will add a fine structure on top of the leading features. Very close to the transition, when the correlation length $\zeta(T)$ reaches the in-plane length scale $1/\sqrt{\lambda}$ at the temperature [38] $T - T_m \sim T_m \ln^{-2}(1/\lambda)$, the three-dimensional effects lead to a full ordering of the system. On general ground, these effects should sharpen the specific-heat cusp in close vicinity of the transition [31,34]. The nature of this three-dimensional order depends on the interlayer interactions: While a simple coupling J' between neighboring layers results in a trivial ferro- ($J' > 0$) or A-type antiferromagnet ($J' < 0$), more complicated helical and fanlike orders can be found if longer-range interactions along z are considered [43,44]. In the latter cases there is the typical in-plane magnetic field scale $B_{3D} = J'/|\boldsymbol{m}|$ aligning the moments in different layers in the same directions and eliminating the magnetic transition.

In conclusion, we have investigated the magnetic transition in $RbEuFe_4As_4$ by specific-heat measurements and by Monte Carlo simulations. The magnetic transition at 14.9 K shifts to lower temperatures in fields along the c axis. This is well reproduced by the simulations of the 2D anisotropic Heisenberg system. This allows us to identify the ab plane as the magnetic easy plane and the specific-heat curve indeed shows a dominant BKT character. A magnetic field normal to the Eu layers shifts the magnetic transition to lower temperature. Applying the field along the Eu planes lifts the rotational symmetry required for a BKT transition. The latter is replaced by a broad crossover from a paramagnetically disordered to a field-ordered state. With a quantitative comparison between our simulation and experimental data, we have extracted the coupling constants $\mathcal{J} = 0.6 \times 10^{-23}$ J/μ_B^2 and the anisotropy $\mathcal{K} = 0.1\mathcal{J}$. The extraction of the phase boundary of the BKT transition and the crossover lines for in- and out-of-plane fields further underline the excellent agreement between experiment and simulations.

The unique feature of $RbEuFe_4As_4$ is that the magnetic transition takes place deep inside the superconducting phase. We expect that the superconductivity has almost no influence on the intralayer exchange interaction between Eu moments and may only modify the interlayer interactions. Therefore, the direct impact of superconductivity on magnetism is likely to be minor. The effects caused by the opposite influence of magnetism on superconductivity are expected to be more pronounced. The presence of the magnetic subsystem with a large susceptibility drastically modifies the macroscopic magnetic response of the superconducting material in the mixed state [45]. The source of the microscopic interaction between the magnetic and superconducting subsystems is an exchange coupling between the Eu moments and Cooper pairs. Even though this coupling is not strong enough to completely destroy superconductivity, such as, e.g., in $ErRh_4B_4$ [46], it may cause a noticeable suppression of superconducting parameters at the magnetic transition. Having established the nature of the robust magnetic order, this work serves as a starting point for further exploring the phenomena related to the influence of magnetism on the superconducting state.

We are thankful for the helpful discussions with Matthew Smylie and Andreas Rydh. This work was supported by the U.S. Department of Energy, Office of Science, Basic Energy Sciences, Materials Sciences and Engineering Division. K.W. and R.W. acknowledge support from the Swiss National Science Foundation through an Early Postdoc Mobility fellowship.

[1] K.-H. Muller and V. N. Narozhnyi, Interaction of superconductivity and magnetism in borocarbide superconductors, Rep. Prog. Phys. **64**, 943 (2001).

[2] M. L. Kulić and A. I. Buzdin, Coexistence of singlet superconductivity and magnetic order in bulk magnetic superconductors and SF heterostructures, in *Superconductivity: Conventional and Unconventional Superconductors*, edited by K. H. Bennemann and J. B. Ketterson (Springer, Berlin, 2008), p. 163.

[3] S. Zapf and M. Dressel, Europium-based iron pnictides: A unique laboratory for magnetism, superconductivity and structural effects, Rep. Prog. Phys. **80**, 016501 (2017).

[4] G. Cao, S. Xu, Z. Ren, S. Jiang, C. Feng, and Z. Xu, Superconductivity and ferromagnetism in $EuFe_2(As_{1-x}P_x)_2$, J. Phys.: Condens. Matter **23**, 464204 (2011); H. S. Jeevan, D. Kasinathan, H. Rosner, and P. Gegenwart, Interplay of antiferromagnetism, ferromagnetism, and superconductivity in $EuFe_2(As_{1-x}P_x)_2$ single crystals, Phys. Rev. B **83**, 054511 (2011).

[5] H. S. Jeevan, Z. Hossain, D. Kasinathan, H. Rosner, C. Geibel, and P. Gegenwart, High-temperature superconductivity in $Eu_{0.5}K_{0.5}Fe_2As_2$, Phys. Rev. B **78**, 092406 (2008).

[6] Y. Qi, Z. Gao, L. Wang, D. Wang, X. Zhang, and Y. Ma, Superconductivity at 34.7 K in the iron arsenide $Eu_{0.7}Na_{0.3}Fe_2As_2$, New J. Phys. **10**, 123003 (2008).

[7] Y. Liu, Y.-B. Liu, Q. Chen, Z.-T. Tang, W.-H. Jiao, Q. Tao, Z.-A. Xu, and G.-H. Cao, A new ferromagnetic superconductor: $CsEuFe_4As_4$, Sci. Bull. **61**, 1213 (2016).

[8] Y. Liu, Y.-B. Liu, Z.-T. Tang, H. Jiang, Z.-C. Wang, A. Ablimit, W.-H. Jiao, Q. Tao, C.-M. Feng, Z.-A. Xu, and G.-H. Cao, Superconductivity and ferromagnetism in hole-doped $RbEuFe_4As_4$, Phys. Rev. B **93**, 214503 (2016).

[9] V. L. Berezinskii, Destruction of long-range order in one-dimensional and two-dimensional systems having a continuous symmetry group. I. Classical systems, Zh. Eksp. Teor. Fiz. **59**, 907 (1971) [Sov. Phys. JETP **32**, 493 (1971)].

[10] J. M. Kosterlitz and D. J. Thouless, Ordering, metastability and phase transitions in two-dimensional systems, J. Phys. C **6**, 1181 (1973).

[11] J. M. Kosterlitz, The critical properties of the two-dimensional xy model, J. Phys. C **7**, 1046 (1974).

[12] K. Hirakawa, H. Yoshizawa, and K. Ubukoshi, Neutron scattering study of the phase transition in two-dimensional planar ferromagnet K_2CuF_4, J. Phys. Soc. Jpn. **51**, 2151 (1982).

[13] K. Hirakawa, Kosterlitz-Thouless transition in two-dimensional planar ferromagnet K_2CuF_4 (invited), J. Appl. Phys. **53**, 1893 (1982).

[14] C. A. Cornelius, P. Day, P. J. Fyne, M. T. Hutchings, and P. J. Walker, Temperature and field dependence of the magnetisation of Rb_2CrCl_4: A two-dimensional easy-plane ionic ferromagnet, J. Phys. C: Solid State Phys. **19**, 909 (1986).

[15] S. Bramwell, P. Holdsworth, and M. Hutchings, Static and dynamic magnetic properties of Rb_2CrCl_4: Ideal 2D-XY behaviour in a layered magnet, J. Phys. Soc. Jpn. **64**, 3066 (1995).

[16] See Supplemental Material at http://link.aps.org/supplemental/10.1103/PhysRevB.99.180502 for a description of the experimental and numerical methods, the anisotropic 2D Heisenberg model, its high-temperature expansion, the scaling of the magnetic correlation, the susceptibility and magnetisation, and the quantitative role of the magnetic anisotropy.

[17] S. Tagliati, V. M. Krasnov, and A. Rydh, Differential membrane-based nanocalorimeter for high-resolution measurements of low-temperature specific heat, Rev. Sci. Instrum. **83**, 055107 (2012).

[18] K. Willa, Z. Diao, D. Campanini, U. Welp, R. Divan, M. Hudl, Z. Islam, W.-K. Kwok, and A. Rydh, Nanocalorimeter platform for *in situ* specific heat measurements and x-ray diffraction at low temperature, Rev. Sci. Instrum. **88**, 125108 (2017).

[19] H. S. Jeevan, Z. Hossain, D. Kasinathan, H. Rosner, C. Geibel, and P. Gegenwart, Electrical resistivity and specific heat of single-crystalline $EuFe_2As_2$: A magnetic homologue of $SrFe_2As_2$, Phys. Rev. B **78**, 052502 (2008).

[20] Z. Ren, Z. Zhu, S. Jiang, X. Xu, Q. Tao, C. Wang, C. Feng, G. Cao, and Z. Xu, Antiferromagnetic transition in $EuFe_2As_2$: A possible parent compound for superconductors, Phys. Rev. B **78**, 052501 (2008).

[21] U. B. Paramanik, P. L. Paulose, S. Ramakrishnan, A. K. Nigam, C. Geibel, and Z. Hossain, Magnetic and superconducting properties of Ir-doped $EuFe_2As_2$, Supercond. Sci. Technol. **27**, 075012 (2014).

[22] A. Oleaga, A. Salazar, A. Thamizhavel, and S. Dhar, Thermal properties and Ising critical behavior in $EuFe_2As_2$, J. Alloys Compd. **617**, 534 (2014).

[23] J. Wosnitza, From thermodynamically driven phase transitions to quantum critical phenomena, J. Low Temp. Phys. **147**, 249 (2007).

[24] M. Bouvier, P. Lethuillier, and D. Schmitt, Specific heat in some gadolinium compounds. I. Experimental, Phys. Rev. B **43**, 13137 (1991).

[25] D. C. Johnston, R. J. McQueeney, B. Lake, A. Honecker, M. E. Zhitomirsky, R. Nath, Y. Furukawa, V. P. Antropov, and Y. Singh, Magnetic exchange interactions in $BaMn_2As_2$: A case study of the J_1-J_2-J_c Heisenberg model, Phys. Rev. B **84**, 094445 (2011).

[26] M. P. Smylie, K. Willa, J.-K. Bao, K. Ryan, Z. Islam, H. Claus, Y. Simsek, Z. Diao, A. Rydh, A. E. Koshelev, W.-K. Kwok, D. Y. Chung, M. G. Kanatzidis, and U. Welp, Anisotropic superconductivity and magnetism in single-crystal $RbEuFe_4As_4$, Phys. Rev. B **98**, 104503 (2018).

[27] V. S. Stolyarov, A. Casano, M. A. Belyanchikov, A. S. Astrakhantseva, S. Y. Grebenchuk, D. S. Baranov, I. A. Golovchanskiy, I. Voloshenko, E. S. Zhukova, B. P. Gorshunov, A. V. Muratov, V. V. Dremov, L. Y. Vinnikov, D. Roditchev, Y. Liu, G. H. Cao, M. Dressel, and E. Uykur, Unique interplay between superconducting and ferromagnetic orders in $EuRbFe_4As_4$, Phys. Rev. B **98**, 140506(R) (2018).

[28] N. Metropolis, A. W. Rosenbluth, M. N. Rosenbluth, A. H. Teller, and E. Teller, Equation of state calculations by fast computing machines, J. Chem. Phys. **21**, 1087 (1953).

[29] W. K. Hastings, Monte Carlo sampling methods using Markov chains and their applications, Biometrika **57**, 97 (1970).

[30] J. Tobochnik and G. V. Chester, Monte Carlo study of the planar spin model, Phys. Rev. B **20**, 3761 (1979).

[31] W. Janke and T. Matsui, Crossover in the XY model from three to two dimensions, Phys. Rev. B **42**, 10673 (1990).

[32] R. Gupta and C. F. Baillie, Critical behavior of the two-dimensional XY model, Phys. Rev. B **45**, 2883 (1992).

[33] A. Cuccoli, V. Tognetti, P. Verrucchi, and R. Vaia, Quantum effects on the Berezinskii-Kosterlitz-Thouless transition in the ferromagnetic two-dimensional XXZ model, Phys. Rev. B **51**, 12840 (1995).

[34] P. Sengupta, A. W. Sandvik, and R. R. P. Singh, Specific heat of quasi-two-dimensional antiferromagnetic Heisenberg models with varying interplanar couplings, Phys. Rev. B **68**, 094423 (2003).

[35] X. F. Wang, T. Wu, G. Wu, H. Chen, Y. L. Xie, J. J. Ying, Y. J. Yan, R. H. Liu, and X. H. Chen, Anisotropy in the Electrical Resistivity and Susceptibility of Superconducting $BaFe_2As_2$ Single Crystals, Phys. Rev. Lett. **102**, 117005 (2009).

[36] W. R. Meier, T. Kong, U. S. Kaluarachchi, V. Taufour, N. H. Jo, G. Drachuck, A. E. Böhmer, S. M. Saunders, A. Sapkota, A. Kreyssig, M. A. Tanatar, R. Prozorov, A. I. Goldman, F. F. Balakirev, A. Gurevich, S. L. Bud'ko, and P. C. Canfield, Anisotropic thermodynamic and transport properties of single-crystalline $CaKFe_4As_4$, Phys. Rev. B **94**, 064501 (2016).

[37] Y. Xiao, Y. Su, W. Schmidt, K. Schmalzl, C. M. N. Kumar, S. Price, T. Chatterji, R. Mittal, L. J. Chang, S. Nandi, N. Kumar, S. K. Dhar, A. Thamizhavel, and T. Brueckel, Field-induced spin reorientation and giant spin-lattice coupling in $EuFe_2As_2$, Phys. Rev. B **81**, 220406(R) (2010).

[38] S. Hikami and T. Tsuneto, Phase transition of quasi-two dimensional planar system, Progr. Theor. Phys. **63**, 387 (1980).

[39] A. Polyakov, Interaction of goldstone particles in two dimensions. Applications to ferromagnets and massive Yang-Mills fields, Phys. Lett. B **59**, 79 (1975).

[40] E. Brézin and J. Zinn-Justin, Renormalization of the Nonlinear σ Model in $2 + \epsilon$ Dimensions—Application to the Heisenberg Ferromagnets, Phys. Rev. Lett. **36**, 691 (1976); Spontaneous breakdown of continuous symmetries near two dimensions, Phys. Rev. B **14**, 3110 (1976).

[41] D. R. Nelson and R. A. Pelcovits, Momentum-shell recursion relations, anisotropic spins, and liquid crystals in $2 + \epsilon$ dimensions, Phys. Rev. B **16**, 2191 (1977).

[42] S. H. Shenker and J. Tobochnik, Monte Carlo renormalization-group analysis of the classical Heisenberg model in two dimensions, Phys. Rev. B **22**, 4462 (1980).

[43] T. Nagamiya, K. Nagata, and Y. Kitano, Magnetization process of a screw spin system, Prog. Theor. Phys. **27**, 1253 (1962).

[44] D. C. Johnston, Magnetic structure and magnetization of helical antiferromagnets in high magnetic fields perpendicular to the helix axis at zero temperature, Phys. Rev. B **96**, 104405 (2017).

[45] V. K. Vlasko-Vlasov, A. E. Koshelev, M. Smylie, J.-K. Bao, D. Y. Chung, M. G. Kanatzidis, U. Welp, and W.-K. Kwok, Self-induced magnetic flux structure in the magnetic superconductor $RbEuFe_4As_4$, Phys. Rev. B **99**, 134503 (2019).

[46] M. B. Maple, H. C. Hamaker, L. D. Woolf, H. B. Mackay, Z. Fisk, W. Odoni, and H. R. Ott, in *Crystalline Electric Field and Structural Effects in f-Electron Systems*, edited by J. E. Crow, R. P. Guertin, and T. W. Mihalisin (Plenum, New York, 1980), pp. 533–543.